JOURNAL OF ENGINEERING SCIENCES

Volume 12, Issue 2 (2025)

*Kermezli T., Announ M., Ladeg S., Douani M. (2025). Experimental design approach to evaluating factors for enhanced cork mass insulation. Journal of Engineering Sciences (Ukraine), Vol. 12(2), pp. F12–F21.* [*https://doi.org/10.21272/jes.2025.12(2).f2*](https://doi.org/10.21272/jes.2025.12(2).f2)


# Experimental Design Approach to Evaluating Factors for Enhanced Cork Mass Insulation

Kermezli T.[1][0000-0002-0899-7568], Announ M.[1*][0000-0002-0621-4806], Ladeg S.[1*][0000-0003-1133-827X], Douani M.[2][0000-0002-9116-2675]

[1] LME Laboratory, Ouzera University Center, University of Medea, 26019 Medea, Algeria;
[2] Faculty of Technology, Hassiba Benbouali University of Chlef, 02180 Chlef, Algeria

| **Article info:** | | |
|---|---|---|
| Submitted: | March 25, 2025 | |
| Received in revised form: | July 9, 2025 | |
| Accepted for publication: | July 15, 2025 | |
| Available online: | July 31, 2025 | |

***Corresponding email:**
kermezli.tayeb@univ-medea.dz

**Abstract.** This research examines the mechanical properties of cork, explicitly focusing on enhancing its mass insulation characteristics by calculating the apparent diffusion coefficient. This coefficient was obtained by combining conductimetric measurements with model calibration and further refined using an optimization model based on the Bat Algorithm. A series of eight experiments was conducted to examine the impact of operating parameters and their interactions on cork's diffusion coefficient using the experimental design according to the response surface methodology. The factors considered included three potential growth areas spread over the North of Algeria, cutting directions, and material states (treated and native). Given the duration and expense of the experiments, a linear model incorporating interactions was employed to examine the effects of all parameters. The Minitab software allowed for estimating the model's coefficients, including interactions, indicating that the diffusion coefficient remains unaffected by the planting area. However, the tangential cutting direction influences the mass insulation property. Additionally, the negative sign of the coefficient associated with thermal heat treatment indicates that this factor enhances cork's insulation performance, reducing the diffusion coefficient from $3.40 \cdot 10^{-12}$ m²/s to $4.57 \cdot 10^{-13}$ m²/s. Moreover, treated cork exhibits a diffusion coefficient value four times lower than that resulting from the tangential cutting direction. As a result, the experimental findings enabled the development of a simplified predictive model for mass diffusivity, with a coefficient of determination of 0.90 and a significance level of 0.05.

**Keywords:** renewable natural material, eco-friendly materials, energy-efficient insulation, response surface methodology, thermal heat treatment.

## 1 Introduction

Cork, a natural material primarily derived from the bark of the cork oak (Quercus suber) [1], is extensively utilized across various fields due to its exceptional cellular properties and chemical composition [2, 3].

To enhance its properties, including the apparent mass diffusion coefficient $D_{app}$, optimal high-temperature thermal heat treatments (THT) were examined by [4].

The samples originate from three distinct geographical growth areas in Algeria, each cut in three specific directions, which can considerably affect the material's mechanical properties [5].

This research employs a systematic approach based on the response surface methodology (RSM) [6]. An experimental investigation is conducted at the LME of the University of Medea, utilizing advanced techniques for the characterization of cork samples.

The main objective is to determine the optimal conditions for minimizing the $D_{app}$, considering the treatment process, geographical areas, and cutting directions.

The procedure involves carefully collecting samples from the three regions, followed by THT treatments according to a pre-established RSM [7]. Analysis of physical and mechanical properties, along with mass diffusion testing [8], is performed accurately for each sample.

This study utilizes a systematic approach to elucidate the impact of thermal treatments on cork $D_{app}$, considering the growth area and cutting directions. The acquired results will contribute not only to the optimization of cork properties for specific applications [9] but also expand the comprehension of the mechanisms governing the behavior of this material, as revealed by [10].

## 2 Literature Review

In recent years, there has been growing interest in cork as a sustainable insulation material, driven by its unique combination of cellular structure, thermal properties, and environmental benefits. Fundamental studies have established critical structure-property relationships, particularly emphasizing the role of suberin content and cellular morphology in determining mechanical and thermal performance [11, 12].

Advanced characterization techniques, including micro-CT scanning and dynamic mechanical analysis, have revealed significant orientation-dependent behavior, with radial and tangential properties differing by as much as 40 % in some cases [13, 14]. This anisotropy has essential implications for insulation applications, where the design must carefully consider directional properties.

Developing predictive models for cork behavior has evolved from classical Fickian diffusion approaches [15] to more advanced computational methods.

Recent work by Santos et al. [16] and Kermezli et al. [17] has quantitatively demonstrated anisotropic diffusion coefficients, providing a foundation for the direction-dependent modeling framework employed in the current study. Parallel advances in metaheuristic optimization techniques have enabled more accurate parameter estimation from experimental data, though challenges remain in accounting for coupled thermal-hygroscopic interactions [18].

While cork is widely utilized in wine stoppers due to its optimal combination of compressibility and gas impermeability [19, 20], its potential in building insulation remains underexploited. Comparative studies highlight cork's superior environmental profile and competitive thermal performance relative to petroleum-based foams, particularly in applications requiring combined thermal and acoustic insulation [4, 5]. However, most existing research has focused on untreated cork, with limited investigation into how controlled thermal modification might enhance performance characteristics for targeted applications.

THT presents both opportunities and challenges for modifying cork. While conventional chemical treatments can be effective, they often degrade mechanical properties, e.g., a 25–30 % reduction in elastic modulus following alkaline processing is observed [10, 21].

Alternative approaches using controlled treatments show promise; preliminary work on beech wood has demonstrated that inert gas environments can effectively modify material properties while minimizing oxidative damage [22, 23].

Based on these findings, a processing protocol can be developed to balance performance enhancement with structural preservation.

Optimizing thermal modification parameters is critical, as demonstrated by Miranda et al. [24], who identified threshold temperatures beyond which structural degradation becomes significant. Their findings showed that steam treatments exceeding 150 °C induce lignin depolymerization, resulting in an 18–22 % increase in brittleness.

These results highlight the importance of temperature control and atmospheric composition, which directly influenced our selection of moderate-temperature (120–140 °C) under oxygen-free processing conditions.

Despite these advances, several key gaps remain in the current understanding of modified cork materials.

First, few studies have systematically examined the coupled thermo-hydro-mechanical behavior under realistic service conditions.

Second, long-term performance data under cyclic environmental loading is notably absent from the literature.

Third, comprehensive life-cycle assessments comparing modified cork to synthetic alternatives are scarce.

The present research addresses these gaps through a combined experimental and modeling approach, introducing an inert-atmosphere thermal modification process while developing a multiscale diffusion model that explicitly accounts for anisotropic effects.

This integrated methodology offers new insights into the property trade-offs between thermal stability and mechanical performance in modified cork materials.

## 3 Materials and Methods

### 3.1 Experimental research

The experimental protocol involves the preparation of natural cork chips sourced from three distinct regions in Algeria (i.e., Jijel, Medea, and Skikda), acquired from the industrial unit. These samples are characterized by high quality [25, 26] and kept in their natural state without prior surface treatment.

The chips are then cut into orthotropic blocks, according to directions, e.g., radial, longitudinal, and tangential (Figure 1), as mentioned by [27], according to specific dimensions that are suitable for the conductimetry method [15].

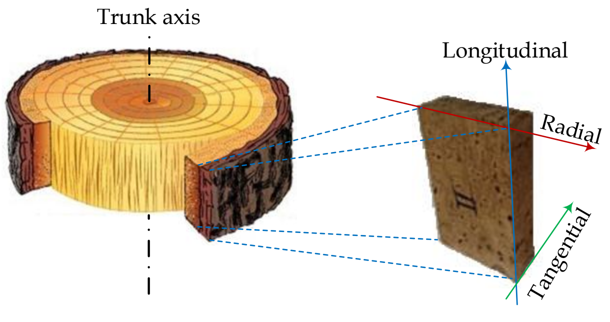


Figure 1 – Different directions of cork cells

Determining the reduced mass involves using thin slabs of cork with an average flat area of $1.934 \cdot 10^{-3}$ m$^2$ and an average thickness of $5.91 \cdot 10^{-3}$ m in the chosen direction.

The samples were subjected to an ecological THT under an inert gas, argon (Ar), to enhance the mechanical properties of the cork.

The thermal cycle was based on the optimal cycle proposed by [15, 18], as shown in Figure 2.

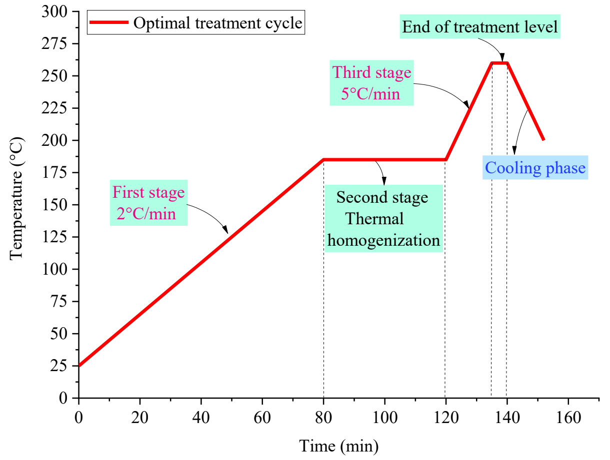


Figure 2 – Heat treatment cycle under inert atmosphere

All cork chips, whether native or treated, consist of 24 elements. The $D_{app}$ value of each chip is directly measured using the conductimetric method, as described by [15].

The principle involves soaking the cork sample in a sodium chloride (NaCl) solution.

Under vacuum, the sample is maintained until saturation is achieved (Figure 3 a).

Subsequently, the sample is immersed in distilled water under agitation to observe the transient molecular diffusion of NaCl using a conductimeter; the instantaneous concentration is recorded by a data acquisition system (Figure 3 b).

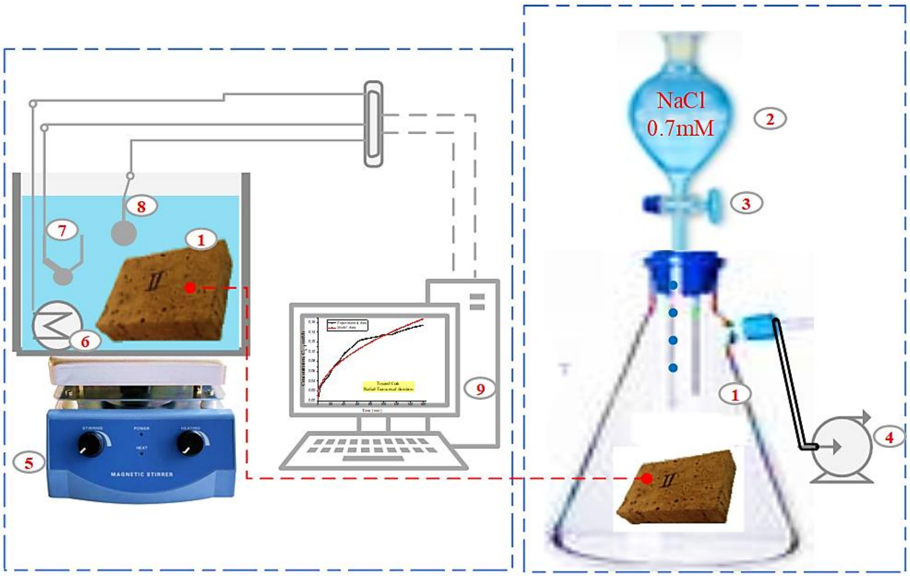


a b

Figure 3 – Schematic of the conductimetric measurement installation: a – transient conductivity measurement; b – impregnation; 1 – cork chip; 2 – funnel; 3 – valve; 4 – vacuum pump; 5 – stirrer; 6 – heat resistance; 7 – thermocouple; 8 – conductimeter; 9 – acquisition system

### 3.2 Numerical calculations

A second-order partial differential equation governs non-steady-state diffusion. Its resolution is analytically complex and typically requires the use of numerical methods.

To simplify the mathematical model, the following simplifying assumptions can be introduced:

1) the diffusion environment does not serve as a site for chemical reactions;

2) the cork chip is non-deformable and homogeneous, with unidirectional diffusion;

3) the concentration has a uniform distribution throughout the sample.

Therefore, the mass balance of equation (1) allows for determining the diffusion fluxes of chemical species within the sample and describing their temporal and spatial evolution.

$$\begin{bmatrix} Accumulation \\ term \end{bmatrix} - \begin{bmatrix} Diffusion \\ term \end{bmatrix} \pm \begin{bmatrix} Production \\ term \end{bmatrix} + \\ + \begin{bmatrix} Convection \\ term \end{bmatrix} = 0. \tag{1}$$

Assuming no chemical reactions and neglecting the negligible contribution of convection, the material balance equation reduces to:

$$\begin{bmatrix} Accumulation \\ term \end{bmatrix} - \begin{bmatrix} Diffusion \\ term \end{bmatrix} = 0. \tag{2}$$

After simplifications, the model is written as follows:

$$\frac{\partial c_i(\zeta,t)}{\partial t} = \frac{1}{\zeta^s}\frac{\partial}{\partial \zeta}\left[\zeta^s D_{app}\frac{\partial c_i(\zeta,t)}{\partial \zeta}\right], \quad (3)$$

where $c_i$ – concentration of the $i$-th chemical species diffusing, mol/m$^3$; $D_{app}$ – the diffusivity coefficient, m$^2$/s; $\zeta$ – coordinate, m; $s$ – power; $t$ – time, s.

In the rectangular coordinate system, adapted to the cork chip, associated with the initial and boundary conditions, the model reduces to:

$$\begin{cases} \frac{\partial c_i(x,t)}{\partial t} = D_{app}\frac{\partial^2 c_i(x,t)}{\partial x^2}; \\ c_i(x,t)\big|_{t=0}^{x>0} = c_{i0}; \\ c_i(x,t)\big|_{t>0}^{x=l} = c_{ip}; \\ \frac{\partial c_i(x,t)}{\partial t}\Big|_{t>0}^{x=0} = 0. \end{cases} \quad (4)$$

Applying the Laplace transform and solving the partial differential equation, the analytical expression of the model representing the reduced mass routine in the form of the concentration of the chemical species in the external medium is given by:

$$\frac{c_i(x,t)-c_{io}}{c_{ip}-c_{io}} = 1 - \frac{4}{\pi}\sum_{n=0}^{\infty}\left\{\frac{(-1)^n}{(2n+1)}cos\left[\frac{(2n+1)\pi x}{2l}\right]\times\right\} \times exp\left[-\frac{(2n+1)^2\pi^2 D_{app}t}{4l^2}\right], \quad (5)$$

where $l$ – the half thickness of the sample.

The calculation of $D_{app}$ on the RSM can be approached through the spatio-temporal analysis of the concentration $c_i(x, t)$ of the diffusing species $i$.

### 3.3 RSM analysis

The three factors in this study were selected based on prior research findings. Orientation significantly affects the thermal properties of natural cork [16]. Moreover, temperature and geographical origin are critical in determining cork's physical structure [28].

Considering that the three factors chosen for this study are entirely qualitative, their impact on the $D_{app}$ was examined using RSM theory, wherein they were abstractly assigned distinct levels when combined [29, 30].

Combining two-by-two factors creates three complete models relating to them. Thus, a full model with three factors and two levels is tested to discern the effect of each factor and the interactions [31].

The general model is revealed to be of linear form:

$$D_{app} = a_0 + a_1x_1 + a_2x_2 + a_3x_3 + a_{12}x_1x_2 + +a_{13}x_1x_3 + a_{23}x_2x_3 + a_{123}x_1x_2x_3 + \varepsilon, \quad (6)$$

where $x_i$ – the $i$-th factor; $a_i$ – the $i$-th influence of factor; $a_{ij}$, $a_{ijk}$ – the higher interactions of factors $i$, $j$, and $k$; $\varepsilon$ – the error.

The respective values of $a_i$, $a_{ij}$, and $a_{ijk}$ are determined via the experiments targeted in the experiment matrix.

It is worth noting that each model is designed to concentrate on two levels and three specific factors by investigating a portion of the factor space to understand their impacts and enhance the interpretation of the obtained results. Consequently, three distinct matrices must be identified to optimally conduct the 24 experiments for estimating the coefficients $a_i$, $a_{ij}$, and $a_{ijk}$ for each combination. The experiment matrix is presented in Table 1, following the method of factor coding [32, 33].

Table 1 – RSM experiment matrix

| Order | $I$ | $x_1$ | $x_2$ | $x_3$ | $x_1x_2$ | $x_1x_3$ | $x_2x_3$ | $x_1x_2x_3$ | $D_{app}$ |
|---|---|---|---|---|---|---|---|---|---|
| 1 | +1 | –1 | –1 | –1 | +1 | +1 | +1 | –1 | $(D_{app})_1$ |
| 2 | +1 | +1 | –1 | –1 | –1 | –1 | +1 | +1 | $(D_{app})_2$ |
| 3 | +1 | –1 | +1 | –1 | –1 | +1 | –1 | +1 | $(D_{app})_3$ |
| 4 | +1 | +1 | +1 | –1 | +1 | –1 | –1 | –1 | $(D_{app})_4$ |
| 5 | +1 | –1 | –1 | +1 | +1 | –1 | –1 | +1 | $(D_{app})_5$ |
| 6 | +1 | +1 | –1 | +1 | –1 | +1 | –1 | –1 | $(D_{app})_6$ |
| 7 | +1 | –1 | +1 | +1 | –1 | –1 | +1 | –1 | $(D_{app})_7$ |
| 8 | +1 | +1 | +1 | +1 | +1 | +1 | +1 | +1 | $(D_{app})_8$ |

The coefficients $a_i$, $a_{ij}$, and $a_{ijk}$ can be evaluated based on the experimental results $(D_{app})_i$ presented in Table 1. In the factor definition section, it is recalled that the study relates to the following combinations:

a) geographical factors (growth areas), namely Jijel, Medea, and Skikda;

b) cutting direction factors (radial, longitudinal, and tangential);

c) State factors relating to the cork samples (native or treated).

The $D_{app}$ value is determined experimentally by the conductimetric method and then adjusted using a model developed in the transient mode.

It should also be noted that interpreting the RSM analysis results, particularly the analysis of the significance of the regression using the ANOVA technique [34, 35], involves repeating the experiments at the points defining the experimental area. However, the use of specific hypotheses considerably simplifies this analysis.

The diffusion coefficient's data acquisition step is conducted using an experimental approach that considers the nature of the cork. According to the factor level, as predicted by the RSM theory, only one sub-sample, consisting of 12 cork chips, was previously treated with THT according to the cycle shown in Figure 2.

It is essential to point out that the order of experimentation is defined by the matrix of experiments, where a complete factorial plan with two levels and three factors [36] has been retained.

Having defined the qualitative experimental factors (planting area, cutting direction, nature (treated or native) on the one hand, and after identifying the experiments to be carried out through the matrix of experiments, they can be enumerated.

Therefore, and for illustrative purposes, the concentration evolution over time is shown for the 3 and 6 orders for each series of experiments, where the results are grouped.

The experiments are subdivided into three sub-groups, defined by three different matrices of experiments, while the interaction between the various factors is analyzed. Two levels were assigned for each factor, defined by their coding as “–1” and “+1”.

## 4 Results

### 4.1 First series of experiments

Table 2 defines the factors and their coding to study their impact on the $D_{app}$ coefficient.

The experimental data relating to the evolution of the NaCl concentration in the aqueous medium can be seen in Figure 4.

Table 2 – 1st-series coding of factors influencing the $D_{app}$ value

| Growth area (A) | Cutting direction (B) | State of the cork chip (C) |
|---|---|---|
| Medea (+1) | Radial (+1) | Treated (+1) |
| Jijel (–1) | Longitudinal (–1) | Native (–1) |

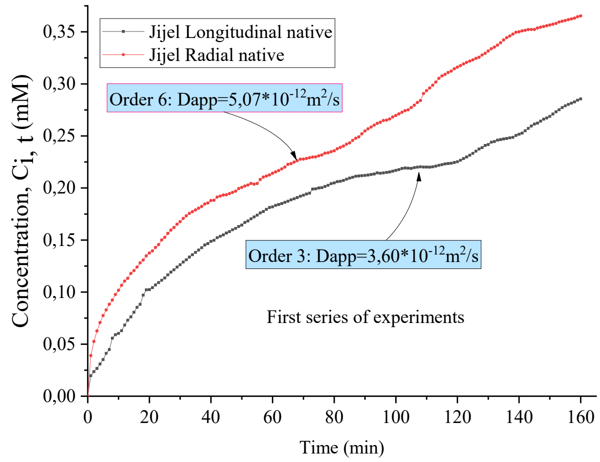


Figure 4 – 1st-series temporal concentration evolution of species $i$ for experiments involving orders 3 and 6

Notably, $D_{app}$ can be estimated by calibrating these experimental results to the analytical solution of the diffusion equation of Fick [37].

The values are presented in Table 3.

Table 3 – 1st-series experimental results of the evolution of the concentration (mM/l) and the $D_{app}$ value

| Order | Time, min | | | | | | | $D_{app}$, $10^{-13}$ m$^2$/s |
|---|---|---|---|---|---|---|---|---|
| | 0 | 5 | 50 | 75 | 100 | 130 | 160 | |
| 1 | 1.08 | 9.84 | 40.15 | 4.63 | 55.39 | 60.73 | 64.25 | 2.62 |
| 2 | 0.79 | 11.73 | 47.68 | 56.70 | 65.15 | 68.48 | 73.94 | 3.93 |
| 3 | 19.69 | 35.14 | 164.36 | 200.06 | 216.89 | 241.71 | 285.60 | 36.00 |
| 4 | 16.77 | 8.20 | 152.08 | 175.25 | 190.43 | 210.52 | 238.99 | 29.00 |
| 5 | 4.97 | 15.93 | 59.18 | 73.79 | 77.11 | 84.61 | 91.14 | 4.57 |
| 6 | 39.04 | 77.48 | 200.55 | 230.90 | 269.72 | 331.61 | 365.26 | 50.70 |
| 7 | 4.86 | 15.71 | 58.52 | 72.99 | 76.28 | 83.71 | 90.17 | 4.50 |
| 8 | 18.98 | 42.39 | 166.67 | 191.90 | 208.50 | 230.38 | 259.75 | 34.00 |

### 4.2 Second series of experiments

Following the exact nature, the coding of the factors in epy second series of experiments can also be followed by monitoring the evolution of the concentrationб as well as the estimated $D_{app}$ coefficient (Table 4, Figure 5).

Table 4 – 2nd-series coding of factors influencing $D_{app}$ value

| Planting area (A) | Cutting direction (B) | Nature of the cork chip (C) |
|---|---|---|
| Medea (+1) | Radial (+1) | Treated (+1) |
| Skikda (–1) | Tangential (–1) | Native (–1) |

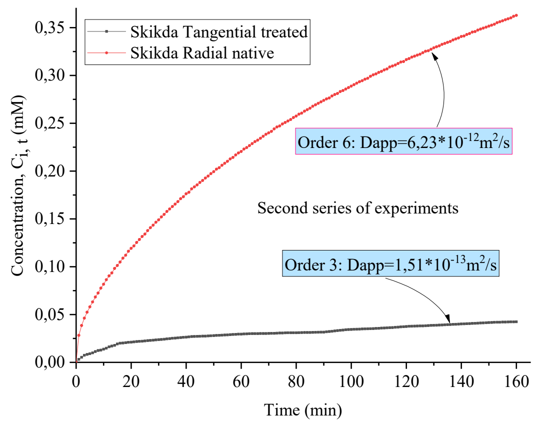


Figure 5 – 2nd-series temporal concentration evolution of species $i$ for experiments involving orders 3 and 6

Table 5 – 2nd-series experimental results of the evolution of the concentration (mM/l) and the $D_{app}$ value

| Order | Time, min | | | | | | | $D_{app}$, $10^{-13}$ m$^2$/s |
|---|---|---|---|---|---|---|---|---|
| | 0 | 5 | 50 | 75 | 100 | 130 | 160 | |
| 1 | 18.98 | 42.39 | 166.67 | 191.90 | 208.49 | 230.38 | 259.48 | 34.00 |
| 2 | 6.68 | 30.03 | 119.45 | 158.96 | 190.86 | 223.42 | 236.24 | 26.00 |
| 3 | 3.18 | 9.05 | 7.99 | 30.66 | 34.41 | 38.76 | 42.43 | 1.51 |
| 4 | 1.73 | 7.46 | 36.81 | 41.86 | 45.34 | 55.75 | 63.56 | 2.10 |
| 5 | 11.39 | 17.71 | 49.35 | 57.98 | 69.34 | 57.98 | 87.50 | 5.95 |
| 6 | 28.26 | 058.06 | 199.37 | 177.75 | 288.78 | 237.16 | 362.78 | 62.30 |
| 7 | 4.97 | 15.93 | 59.18 | 073.79 | 77.11 | 84.61 | 91.14 | 4.57 |
| 8 | 1.47 | 38.11 | 129.30 | 152.59 | 172.99 | 195.55 | 222.75 | 22.50 |

## 4.3 Third series of experiments

This series of experiments is intended to complete the analysis of the effect of the factors outlined in this study on the $D_{app}$.

Similarly, Figure 6 and Tables 6–7 illustrate the coding of factors and changes in concentration, as well as the optimized $D_{app}$ obtained from using the Bat algorithm [38, 39].

Table 6 – 3rd-series coding of factors influencing $D_{app}$ value

| Planting area (A) | Cutting direction (B) | Nature of the cork chip (C) |
|---|---|---|
| Jijel (+1) | Longitudinale (+1) | Traité (+1) |
| Skikda (–1) | Tangentielle (–1) | Natif (–1) |

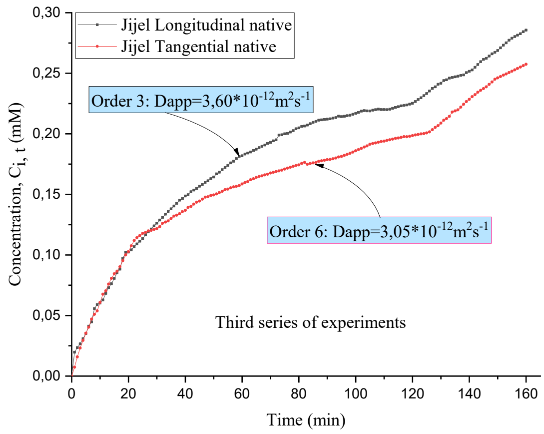


Figure 6 – 3rd-series temporal concentration evolution of species *i* for experiments involving orders 3 and 6

Table 7 – 3rd-series experimental results of the evolution of the concentration (mM/l) and the $D_{app}$ value

| Order | Time, min | | | | | | | $D_{app}$, $10^{-13}$ m$^2$/s |
|---|---|---|---|---|---|---|---|---|
| | 0 | 5 | 50 | 75 | 100 | 130 | 160 | |
| 1 | 17.47 | 38.11 | 129.30 | 152.59 | 173.00 | 195.55 | 222.75 | 22.50 |
| 2 | 0.90 | 7.53 | 27.91 | 31.08 | 38.83 | 41.96 | 43.85 | 1.17 |
| 3 | 19.70 | 35.14 | 164.36 | 200.06 | 216.89 | 241.71 | 285.60 | 36.00 |
| 4 | 14.52 | 45.29 | 153.50 | 177.75 | 213.07 | 237.16 | 263.71 | 51.90 |
| 5 | 1.08 | 9.84 | 40.15 | 46.31 | 55.39 | 60.73 | 64.25 | 2.62 |
| 6 | 7.32 | 35.39 | 149.55 | 170.90 | 185.96 | 208.88 | 257.43 | 30.50 |
| 7 | 4.47 | 12.12 | 51.243 | 57.98 | 62.63 | 76.72 | 80.80 | 4.12 |
| 8 | 3.18 | 9.05 | 27.99 | 30.66 | 34.41 | 38.76 | 42.43 | 1.51 |

## 4.4 1st-model's impact of factors on $D_{app}$

Investigating the effects of the factors and their higher-order interactions necessitates calculating the coefficients $a_i$, $a_{ij}$, and $a_{ijk}$ for each experimental series, as well as a variance analysis to determine the significance of the established regression. The Minitab software was used for this purpose.

For the first series of experiments and the coded factors, Minitab produced the following regression.

Within the 1st model,

$$D_{app} = 20.660 - 2.790 \cdot A + 2.778 \cdot B - 16.760 \cdot C + \\ +3.135 \cdot A \cdot C - 2.148 \cdot B \cdot C + 1.056 \cdot A \cdot B \cdot C. \quad (7)$$

According to RMS theory, interactions of order greater than or equal to three can be neglected (hypothesis 1). The interaction of factors *A*, *B*, and *C* is ignored. It follows that any effect or interaction whose coefficient is of the same order of magnitude as the coefficient of the interaction of order is automatically neglected, which makes the interaction between A and B insignificant. This leads to

$$D_{app} = 20.66 - 2.79 \cdot A + 2.78 \cdot B - 16.76 \cdot C + \\ +3.14 \cdot A \cdot C - 2.15 \cdot B \cdot C. \quad (8)$$

The regression equation can be simplified according to hypothesis 5, which contends that interaction is generally weak when it involves a weak main factor with a strong main factor.

Upon analysis, it is indicated that factor *C* has a substantial absolute value, and considering the analytical expression of the $D_{app}$, it can be concluded that all interactions of the factors with *C* can potentially be neglected.

The regression is thus simplified to:

$$D_{app} = 20.66 - 2.79 \cdot A + 2.78 \cdot B - 16.76 \cdot C. \quad (9)$$

This simplification reveals that the effects or interactions with an influence are approximately null.

This analysis of significance leads to the following final expression:

$$D_{app} = 20.66 - 16.76 \cdot C. \quad (10)$$

Based on the variance analysis (ANOVA) results, a more thorough analysis should be conducted following the repeated experiments outlined in the experiment matrix.

This simplification is justified by comparing the regression coefficients presented in the Pareto chart (Figure 7).

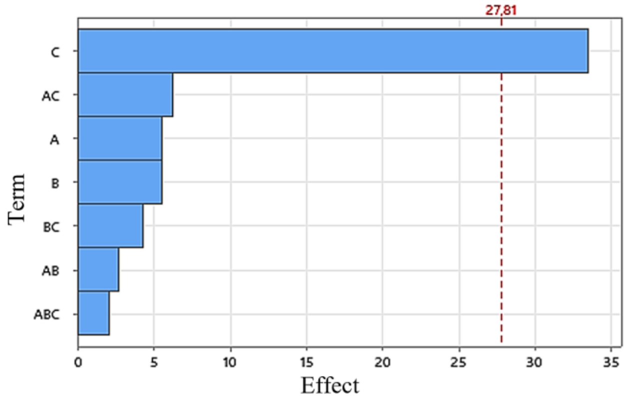


Figure 7 – 1st model's Pareto chart

## 4.5 2nd-model's impact of factors on *D<sub>app</sub>*

Within the 2nd model,

$$D_{app} = 19.87 - 3.20 \cdot A + 6.84 \cdot B - 16.33 \cdot C - \\ -4.22 \cdot A \cdot B + 3.0 \cdot A \cdot C - 5.11 \cdot B \cdot C + 3.73 \cdot A \cdot B \cdot C. \quad (11)$$

The following conclusions regarding higher-order interactions and influencing factors can be drawn based on the abovementioned assumptions. Initially, the insignificance of third-order interactions simplifies the model. Secondly, the area has a low influence, as its coefficients are inferior to those of the triple interactions.

The *C* factor (treatment) is essential, and the influence of the direction is also significant, especially concerning the tangential direction.

According to hypothesis 5, the interaction between weak and strong factors is classified as weak. The interaction between the state and the growth area is thus eliminated.

The remaining factors include direction, characterized by a tangential coefficient of "–1", and the state, which is also associated with a treatment value of "–1".

Furthermore, an interaction has been noted between the growth area and direction (specifically tangential in the case of the Skikda area), along with an interaction between the direction and state (radial, treated) as shown in Figure 8.

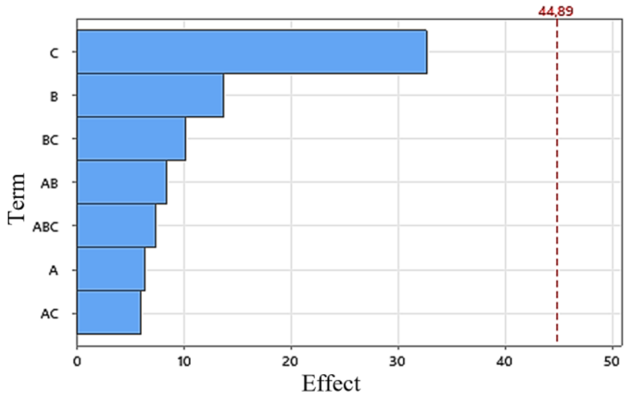


Figure 8 – 2nd model's Pareto chart

The regression equation is expressed as follows:

$$D_{app} = 19.87 + 6.84 \cdot B - 16.33 \cdot C - \\ -4.22 \cdot A \cdot B - 5.11 \cdot B \cdot C. \quad (12)$$

## 4.6 3rd-model's impact of factors on $D_{app}$

Within the 3rd model,

$$D_{app} = 18.79 - 1.22 \cdot A + 4.87 \cdot B - 16.43 \cdot C - \\ -3.13 \cdot A \cdot B + 0.76 \cdot A \cdot C - 3.86 \cdot B \cdot C + 2.84 \cdot A \cdot B \cdot C. \quad (13)$$

In this third set of regressions, it can be observed that triple interactions are insignificant, resulting in the simplification of the developed model. The influence of the growth area and state-growth area interactions is negligible, consistent with the fifth hypothesis.

This set of analyses confirmed the treatment's impact on the diffusion coefficient (Figure 9).

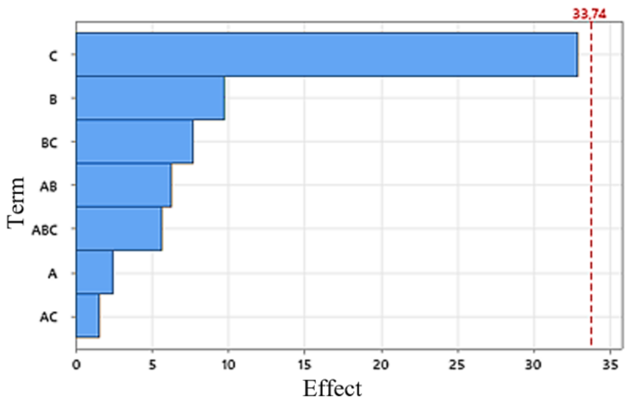


Figure 9 – 3rd model's Pareto chart

The impact of the tangential direction is considerable. In conclusion, the treatment and direction are essential factors to consider when analyzing differences in the diffusion coefficient. This expert interpretation highlights the main findings of this investigation.

$$D_{app} = 18.79 + 4.87 \cdot B - 16.43 \cdot C - 3.86 \cdot B \cdot C. \quad (14)$$

This investigation reveals that the analysis of these analytical expressions, i.e., equations (10), (12), and (14), shows the following. Neither the growth area nor its interactions significantly affect the diffusion coefficient.

On the other hand, the tangential cutting direction is more proper for insulation, as it gives a lower $D_{app}$.

The negative sign of the effect of the treatment indicates that it leads to a four-fold improvement in insulation. As for the interaction of the cutting direction and the state of the material (native or treated) on the $D_{app}$ coefficient, the negative sign of the $B \cdot C$ coefficient suggests that the lowest $D_{app}$ coefficients are obtained when factors $B$ and $C$ have both conditions, confirming conclusions 2 and 3.

Overall, in this research, the interactions between factors $A$, $B$, and $C$ were examined, as well as their effects on the diffusion coefficient.

Firstly, the triple interactions were found to be negligible, which simplifies our model. Secondly, the state of the cork (factor $C$) emerged as a dominant element. Its interactions with the weaker factors A and B were considered insignificant. On the other hand, the effect of treatment on the diffusion coefficient was significant.

It is essential to consider treatment and direction to understand variations in the diffusion coefficient.

## 5 Discussion

The modeling approach adopted in this study is based on several simplifying assumptions: cork is considered a homogeneous, non-deformable material, and the model excludes potential chemical interactions and anisotropic swelling, particularly in thermally treated samples. Hygroscopic properties were estimated using data from structurally analogous materials (e.g., wood), incorporating measurements of relative humidity, mass loss, dimensional stability, and density [40].

The analytical solution employed is simplified and does not account for moisture exchange dynamics or long-term aging effects, as observed in polymer composites [41].

To improve the accuracy and predictive power of $D_{app}$ estimations, future models should integrate thermogravimetric analysis, porosity, and detailed hygroscopic behavior.

Future studies should also investigate the effects of cyclic humidity, UV exposure, and combined thermal–mechanical loading on diffusion behavior. Machine learning methods like artificial neural networks and support vector machines may offer promising tools for predicting $D_{app}$ in heterogeneous material systems.

Comparative analyses with other eco-friendly insulating materials (e.g., hemp or flax) could further contextualize cork's performance within the broader class of bio-based alternatives.

By integrating advanced modeling techniques and exploring alternative bio-based resources, upcoming research may expand the applicability of cork in sustainable construction and energy-efficient design. Such multidisciplinary efforts will reinforce cork's status as a renewable, competitive insulation material within global environmental and sustainability goals.

## 6 Conclusions

The fields of research and development are focused on carrying out the insulation of products or materials that meet environmental rules against pollution. In this perspective, cork was chosen as the material of choice, given its properties and availability in Algeria. Because numerous quantitative factors influence cork quality in terms of insulation, the complete factorial model of RMS theory was used to analyze the impact of the main effects and their interactions on the diffusion coefficient.

Due to the investigation's complexity, the growth area's impact on the properties was considered. For this purpose, three fairly spread areas over northern Algeria were chosen, where samples of native cork were selected and cut in three different directions (radial, tangential, and longitudinal).

Some of these samples were treated at high temperatures and subjected to a boiling process. Using the conductometric method and based on Fick's second law, the apparent diffusion coefficient was approximated and refined by using the Bat algorithm.

For a significance level of 0.05 and based on the analysis of the significance of the factors and their interactions, the study highlighted the importance of the dual interactions between the growth area and the direction, as well as between the direction and the state of the material, while highlighting the complexity of the relationships between the various factors. Thus, it emerged that:

Thermal heat treatment significantly improves the apparent diffusion coefficient $D_{app}$ of the cork obtained, from $3.40 \cdot 10^{-12}$ m$^2$/s to $4.57 \cdot 10^{-13}$ m$^2$/s (a reduction of 13 times). The cutting direction most favorable to the production of insulating material is the tangential cut $D_{JTn} = 3.05 \cdot 10^{-12}$ m$^2$/s, compared with the other two cutting directions ($5.07 \cdot 10^{-12}$m$^2$/s, $3.60 \cdot 10^{-12}$ m$^2$/s).

The cork from Jijel stands out for its better mass insulation due to the low value of the coefficient $D_{JTt} = 1.17 \cdot 10^{-13}$ m$^2$/s, lower than those from Medea ($D_{MTt} = 2.10 \cdot 10^{-13}$ m$^2$/s) and Skikda ($D_{STt} = 1.51 \cdot 10^{-13}$ m$^2$/s), respectively.

The investigation using the response surface method showed that, regardless of the growth area and the cutting direction, the samples subjected to thermal heat treatments have reduced their diffusivity by ten times compared to the native cork. For this reason, the heat treatment technique is chosen as the main enhancement factor in the quality of cork intended for insulation purposes. The mathematical model developed in this study is powerful for predicting the value of the $D_{app}$ with high accuracy.

## References


1. Sen, A., Zhianski, M., Glushkova, M., Petkova, K., Ferreira, J., Pereira, H. (2016). Chemical composition and cellular structure of corks from Quercus suber trees planted in Bulgaria and Turkey. *Wood Science and Technology*, Vol. 50, pp. 1261–1276. https://doi.org/10.1007/s00226-016-0836-y
2. Anjos, O., Rodrigues, C., Morais, J., Pereira, H. (2014). Effect of density on the compression behaviour of cork. Materials & Design, Vol. 53, pp. 1089–1096. https://doi.org/10.1016/j.matdes.2013.07.038
3. Anjos, O., Pereira, H., Rosa, E. (2008). Effect of quality, porosity and density on the compression properties of cork. *Holz als Roh-und Werkstoff*, Vol. 66, pp. 295–301. http://hdl.handle.net/10400.5/5608
4. Zemirline, A., Kermezli, T., Announ, M., Douani, M. (2022). Investigation of the effect of cutting directions on the improvement of mechanical parameters of treated cork by THT: Experimental measurement, modelling and optimization of mass transfer. *Mechanika*, Vol. 28(3), pp. 204–210. https://doi.org/10.5755/j02.mech.26956
5. Silva, S.P., Sabino, M.A., Fernandes, E.M., Correlo, V.M., Boesel, L.F., Reis, R.L. (2005). Cork: properties, capabilities and applications. *International Materials Reviews*, Vol. 50(6), pp. 345–365. https://doi.org/10.1179/174328005X41168
6. Kincl, M., Turk, S., Vrečer, F. (2005). Application of experimental design methodology in development and optimization of drug release method. International *Journal of Pharmaceutics*, Vol. 291(1–2), pp. 39–49. https://doi.org/10.1016/j.ijpharm.2004.07.041
7. Lagorce-Tachon, A., Karbowiak, T., Champion, D., Gougeon, R.D., Bellat, J.-P. (2015). Mechanical properties of cork: effect of hydration. *Materials & Design*, Vol. 82, pp. 148–154. https://doi.org/10.1016/j.matdes.2015.05.034
8. Prades, C., Gómez-Sánchez, I., García-Olmo, J., González-Hernández, F., González-Adrados, J.R. (2014). Application of VIS/NIR spectroscopy for estimating chemical, physical and mechanical properties of cork stoppers. *Wood Science and Technology*, Vol. 48, pp. 811–830. https://doi.org/10.1007/s00226-014-0642-3
9. Pereira, H. (2015). The rationale behind cork properties: A review of structure and chemistry. *BioResources*, Vol. 10(3), pp. 6207–6229. https://doi.org/10.15376/biores.10.3.Pereira
10. Pereira, H., Graça, J., Baptista, C. (1992). The effect of growth rate on the structure and compressive properties of cork. *IAWA Journal*, Vol. 13(4), pp. 389–396. https://doi.org/10.1163/22941932-90001294
11. Petlitckaia, P., Toussaint, B., Paul-Antoine, S., Yann, Q. (2024). Valorization of virgin cork by the design of cork-plaster composites. *Inorganic Chemistry Communications*, Vol. 161, 111782. https://doi.org/10.1016/j.inoche.2023.111782
12. Gürgen, S. (2024). Sustainability of cork and protective systems. *In: Gürgen, S. (eds) Guarding with Cork: A Sustainable Solution for Protection*, pp. 1–17. Springer, Cham, Switzerland. https://doi.org/10.1007/978-3-031-72882-2_1
13. Dymek, M., Ptak, M., Kaczyński, P., Fernandes, F.A.O., de Sousa, R.J.A., Serra, G.F., Kurańska, M. (2024). Eco-friendly cork–polyurethane biocomposites for enhanced impact performance: experimental and numerical analysis. *Polymers*, Vol. 16(7), 887. https://doi.org/10.3390/polym16070887
14. Choi, J.-S., Woo, B.-H., Kim, H.-G., Kim, J.-Y., Ryou, J.-S. (2025). Possibility investigation of phase change material-impregnated and surface coated cork as an aggregate for building envelope application. *Advances in Building Energy Research*, Vol. 19(2), pp. 241–267. https://doi.org/10.1080/17512549.2025.2451359
15. Kermezli, T., Bensmaili, A., Amokrane, K., Gacemi, A. (2013). Mechanical behavior of cork modified by heat treatment at high temperature. *Mechanika*, Vol. 19(4), pp. 424–428. https://doi.org/10.5755/j01.mech.19.4.5053
16. Santos, T., Amaral, J.S., Amaral, V.S., Costa, V.A.F. (2025). In-plane thermal anisotropy of natural cork and its variability. *Measurement*, Vol. 242, 116062. https://doi.org/10.1016/j.measurement.2024.116062
17. Kermezli, T., Announ, M., Boukrida, B., Douani, M. (2025). Prediction by artificial neural network of insulation performance of ecotreated cork stoppers: Experimental measurement, modeling and optimization. *Edelweiss Applied Science and Technology*, Vol. 9(4), pp. 3082–3093. https://doi.org/10.55214/25768484.v9i4.6738
18. Boukrida, B., Kermezli, T., Announ, M., Douani, M. (2023). Improvement of cork insulating properties using ecological treatment with prediction of the diffusion coefficient by ANN approach, under the effect of the area and the direction of the cut. *Journal of Advanced Research in Fluid Mechanics and Thermal Sciences*, Vol. 109(1), pp. 177–187. https://doi.org/10.37934/arfmts.109.1.177187
19. Leleu, G., Garcia, L., de Moura, P.H.B., Da Costa, G., Saucier, C., Richard, T. (2025). Cork impact on red wine aging monitoring through $^{1}$H NMR metabolomics: A comprehensive approach. *Food Research International*, Vol. 203, 115772. https://doi.org/10.1016/j.foodres.2025.115772
20. Rives, J., Fernandez-Rodriguez, I., Rieradevall, J., Gabarrell, X. (2011). Environmental analysis of the production of natural cork stoppers in southern Europe (Catalonia – Spain). *Journal of Cleaner Production*, Vol. 19(2–3), pp. 259–271. https://doi.org/10.1016/j.jclepro.2010.10.001
21. Gerometta, M., Gabrion, X., Lagorce, A., Villette, F., Thibaud, S., Karbowiak, T. (2025). Influence of water and ethanol vapours on the compressive behaviour of natural cork during ageing. *Industrial Crops and Products*, Vol. 233, 121333. https://doi.org/10.1016/j.indcrop.2025.121333

22. Lo Giudice, V., Antov, P., Koynov, D., Kristak, L., Lee, S.H., Lubis, M.A.R., Mecca, M., Moretti, N., Tiwari, R., Todaro, L. (2023). Effect of thermo-vacuum modification on selected chemical, physical, and mechanical properties of Siberian larch (Larix sibirica L.) wood. *Wood Material Science & Engineering*, Vol. 18(6), pp. 1991–2000. https://doi.org/10.1080/17480272.2023.2212253
23. Kozakiewicz, P., Laskowska, A., Drożdżek, M., Zawadzki, J. (2022). Influence of Thermal modification in nitrogen atmosphere on physical and technological properties of European wood species with different structural features. *Coatings*, Vol. 12(11), 1663. https://doi.org/10.3390/coatings12111663
24. Miranda, I., Lourenço, A., Sousa, V., Cardoso, A., Pereira, H. (2025). Weathering impact on expanded cork agglomerates as simulated by artificial UV light irradiation. *International Journal of Environmental Science and Technology*, pp. 1–10. https://doi.org/10.1007/s13762-025-06552-9
25. Graça, J., Pereira, H. (2004). The periderm development in Quercus suber. *IAWA Journal*, Vol. 25(3), pp. 325–335. https://doi.org/10.1163/22941932-90000369
26. Paulo, J.A., Santos, D.I. (2023). Virgin cork colour and porosity as predictors for secondary cork industrial quality. Industrial Crops and Products, Vol. 205, 117513. https://doi.org/10.1016/j.indcrop.2023.117513
27. Miranda, I., Gominho, J., Pereira, H. (2013). Cellular structure and chemical composition of cork from the Chinese cork oak (Quercus variabilis). *Journal of Wood Science*, Vol. 59, pp. 1–9. https://doi.org/10.1007/s10086-012-1300-8
28. Jové, P., de Nadal, R., Verdum, M., Fiol, N. (2025). Characterisation of cork volatile organic compounds using TD-GC-MS: effects of origin, washing process, and thermal processing of cork stoppers. *Processes*, Vol. 13(5), 1505. https://doi.org/10.3390/pr13051505
29. Mäkelä, M. (2017). Experimental design and response surface methodology in energy applications: A tutorial review. *Energy Conversion and Management*, Vol. 151, pp. 630–640. https://doi.org/10.1016/j.enconman.2017.09.021
30. Megahed, S.M., Habib, A.A., Hammad, S.F., Kamal, A.H. (2021). Experimental design approach for development of spectrofluorimetric method for determination of favipiravir; a potential therapeutic agent against COVID-19 virus: Application to spiked human plasma. *Spectrochimica Acta Part A: Molecular and Biomolecular Spectroscopy*, Vol. 249, 119241. https://doi.org/10.1016/j.saa.2020.119241
31. Cho, I.-H., Zoh, K.-D. (2007). Photocatalytic degradation of azo dye (Reactive Red 120) in $TiO_2$/UV system: Optimization and modeling using a response surface methodology (RSM) based on the central composite design. *Dyes and Pigments*, Vol. 75(3), pp. 533–543. https://doi.org/10.1016/j.dyepig.2006.06.041
32. Lucas, J.M. (2010). Response surface methodology: Process and product optimization using designed experiments. *Journal of Quality Technology*, Vol. 42(2), pp. 228–230. https://doi.org/10.1080/00224065.2010.11917819
33. Ahmad, K., Ghatak, H.R., Ahuja, S.M. (2022). Optimal production of vanillin and 4-hydroxybenzaldehyde from rice straw hydrolysis residue (RSHR) over $TiO_2$/UV and ZnO/UV system. *Journal of the Indian Chemical Society*, Vol. 99(3), 100382. https://doi.org/10.1016/j.jics.2022.100382
34. Koh, J.E., Ooi, C.P., Lim-Ashworth, N.S., Vicnesh, J., Tor, H.T., Lih, O.S., Tan, R.-S., Acharya, U.R., Fung, D.S.S. (2022). Automated classification of attention deficit hyperactivity disorder and conduct disorder using entropy features with ECG signals. *Computers in Biology and Medicine*, Vol. 140, 105120. https://doi.org/10.1016/j.compbiomed.2021.105120
35. Khan, S.A., Imran, M., Ali, B., Muhammad, T. (2025). Towards a new strategy modelling to optimise thermal and solutal transportations within a magnetised blood-based hybrid nanofluid flow over gyrating sphere. *International Journal of Ambient Energy*, Vol. 46(1), 2444328. https://doi.org/10.1080/01430750.2024.2444328
36. Liu, M., Sharma, M., Lu, G.-L., Zhang, Z., Yin, N., Wen, J. (2023). Full factorial design, physicochemical characterization, ex vivo investigation, and biological assessment of glutathione-loaded solid lipid nanoparticles for topical application. *International Journal of Pharmaceutics*, Vol. 630, 122381. https://doi.org/10.1016/j.ijpharm.2022.122381
37. Deng, Y., Zhao, S., Yang, X., Guo, H., Li, Y., Xu, W., Chen, J., Wang, Z., Guo, M., Liu, D. (2021). Novel accelerated penetration extraction for polyphenol extraction from pomegranate skins: utilization of Fick's law. *ACS Sustainable Chemistry & Engineering*, Vol. 9(10), pp. 3702–3709. https://doi.org/10.1021/acssuschemeng.0c08013
38. Al-Betar, M.A., Awadallah, M.A. (2018). Island bat algorithm for optimization. *Expert Systems with Applications*, Vol. 107, pp. 126–145. https://doi.org/10.1016/j.eswa.2018.04.024
39. Yuvapriya, T., Lakshmi, P., Elumalai, V.K. (2023). Experimental validation of LQR weight optimization using bat algorithm applied to vibration control of vehicle suspension system. *IETE Journal of Research*, Vol. 69(11), pp. 8142–8152. https://doi.org/10.1080/03772063.2022.2039079
40. Elrhayam, Y., El Bachiri, A. (2024). Study of the effect of heat temperature on the chemical changes and hygroscopicity of eucalyptus wood by FT-IR and prediction of mechanical properties by the MLR regression method. *Spectrochimica Acta Part A: Molecular and Biomolecular Spectroscopy*, Vol. 321, 124576. https://doi.org/10.1016/j.saa.2024.124576
41. Starkova, O., Aiello, M.A., Aniskevich, A. (2023). Long-term moisture diffusion in vinylester resin and CFRP rebars: A 20-year case study. *Composites Science and Technology*, Vol. 242, 110167. https://doi.org/10.1016/j.compscitech.2023.110167